PROCEEDINGS OF SPIE

SPIEDigitalLibrary.org/conference-proceedings-of-spie

Tailoring the shape of oxide complex nanostructures

B. Méndez, I. López, M. Alonso-Orts, A. Sanz, E. Nogales, et al.

SPIE.

Tailoring the shape of oxide complex nanostructures

B. Méndez*[a], I. López[a,b], M. Alonso-Orts[a], A. Sanz[a], E. Nogales[a], P. Hidalgo[a], J. Piqueras[a]
[a]Dept. Física de Materiales, Universidad Complutense de Madrid, Madrid 28040, Spain
[b]Istituto Nazionale di Ottica (INO)-CNR, via Carrara 1, 50019 Sesto Fiorentino FI, Italy

ABSTRACT

The synthesis of complex nanostructures that combine materials and dimensionality, promises the ability to identify novel designs and architectures with enhanced properties that could be used in new devices. One of the building blocks in nanomaterials are nanowires, which offer several possibilities to get complex nanostructures. We present two kinds of morphologies based on oxide nanowires obtained by a thermal evaporation method. The common feature of both morphologies is a central oxide nanowire and, depending on the growth parameters, nanowires with either nanocrystallites or nano/microrods attached to the central wire are obtained. We have previously reported the fabrication of several single oxide nanowires and in particular, gallium oxide (β-Ga_2O_3) and zinc germanate oxide (Zn_2GeO_4) nanowires. Here we report the shape evolution of these nanowires by the suitable modification of the growth parameters. The addition of tin oxide (SnO_2) to the precursors and variation of the thermal treatments duration result in the formation of the above-mentioned complex nanostructures. Structural and chemical characterizations were performed by electron microscopy techniques and Raman spectroscopy. The results shed light on the understanding of the driving mechanisms that lead to the formation of complex oxide nanostructures.

Keywords: semiconducting oxide nanowires, gallium and tin oxide, germanates nanowires, electron microscopy, thermal evaporation method, Raman spectroscopy

1. INTRODUCTION

From the point of view of novel device technologies, nanowires elements can be considered as one of the main building blocks in innovative assemblies. The reason is the strong interest in going beyond planar technologies, where thin films are the main actors, and alternative designs as vertical ones where nanowires play a key role[1]. Nanowires offer several possibilities to get complex nanostructures, such as core-shell, branched wires, crossing wires or hierarchical structures, to name a few[2]. Moreover, nanowires could act as scaffolds or substrates for other nanomaterials, such as nanoparticles or ultrathin layers, what could widen the range of applications. Semiconducting oxide materials are attractive in the field of optoelectronics because of merging optical transparency and suitable electronic conductivity. In addition, their wide band gap character enables further applications in the ultraviolet range and in high power devices. Finally, their chemical stability and good mechanical properties make oxides an attractive choice for a number of applications[3]. In this work, we report on complex oxide nanostructures based on Ga_2O_3, SnO_2, and Zn_2GeO_4, which have energy band gaps of 4.9 eV, 3.6 eV and 3.3 eV, respectively.

A variety of synthesis routes to obtain oxide nanowires have been reported, being thermal evaporation method a rather simple one that enable to grow both undoped and doped materials. We have successfully fabricated several oxide nanowires by simple evaporation-solidification mechanism[4-8]. The key parameters that control the growth process are the temperature, the duration, the gas flow and the source materials. Any action over any of these factors may alter the final product, not only in their physical properties but also in the final morphology or architecture. In particular, suitable doping and orientation of Ga_2O_3 nanowires have been revealing as the driven mechanism to achieve complex Ga_2O_3/SnO_2 nanostructures[9-10]. In this paper, we report on the shape evolution of complex nanostructures based on nanowires by suitable modification of the growth parameters. In particular, we report on heterostructures formed by Ga_2O_3 and Zn_2GeO_4 nanowires as the main axis, with either modulated diameter or with nanocrystallites attached to the axis.

*bianchi@ucm.es; phone +34 91 394 4746; fax -34 91 394 4547; finegroup.es

Nanotechnology VIII, edited by Ion M. Tiginyanu, Proc. of SPIE Vol. 10248, 1024805
 · doi: 10.1117/12.2264457

2. EXPERIMENTAL

A pellet of a mixture of Ga_2O_3 and SnO_2 compacted powders in a weight ratio (90%:10%) was used as substrate where Ga chips were placed onto it. The pellet was treated for 15 hours at 1500ºC under an argon flow of 0.8 l/min and a huge amount of nanostructures was formed. Alternatively, a small amount of Cr impurities was added to the previous precursors, which results in changes in the final morphology of the Ga_2O_3/SnO_2 nanostructures. On the other hand, we have previously reported the growth of undoped Zn_2GeO_4 nanowires by using a compacted pellet made of a mixture of ZnO, Ge and carbon powders with a weight ratio 2:1:2 that acted as source and as substrate[6]. The thermal treatment was carried out at 800 ºC for 8 hours. In this work, complex Zn_2GeO_4/SnO_2 nanostructures were obtained by adding a 10 % of SnO_2 to the mixture {ZnO+Ge} and followed the same thermal treatment as in Ref. 6.

The morphology was analyzed in a Leica 440 Steroscan scanning electron microscope (SEM) while spatially resolved chemical composition was studied in the energy dispersive X-ray microanalysis (EDS) mode. Luminescence was analyzed both by Cathodoluminescence (CL) in the SEM and by photoluminescence (PL) in an optical confocal microscope (Horiba Jobin Ybon LabRam HR800). The confocal microscope was equipped with an ultraviolet laser (λ = 325 nm) and enables as well to carry out Raman spectroscopy.

3. RESULTS AND DISCUSSION

Complex Ga_2O_3/SnO_2 and Zn_2GeO_4/SnO_2 micro- and nanostructures have been grown in a single step thermal treatment, via a vapor-solid (VS) mechanism. Figure 1a shows the SEM image and the {Ga + Sn} elemental mapping of a representative complex oxide nanostructure composed by a main Ga_2O_3 nanowire with attached SnO_2 particles. The Ga_2O_3 axis width is around 200 nm and the size of the SnO_2 particles is about 1 µm. It is worth mentioning that Ga_2O_3 has a monoclinic lattice structure while SnO_2 is of rutile phase. However, TEM measurements have revealed that a good lattice matching between both lattices[10]. In addition, we have explored the possibility to obtain this kind of morphology with other semiconducting oxides. Zn_2GeO_4 nanowires are obtained by using a mixture of ZnO:Ge:carbon in a 2:1:2 weight ratio as source and substrate[6]. In this case, a 10% of SnO_2 was incorporated to the mixture. Figure 1b shows that a similar complex structure with particles around an axis is formed. Figure 1c shows the elemental mappings for Zn, Ge and Sn of a Zn_2GeO_4 nanowire decorated with SnO_2 particles, which are doped with Ge and Zn. The SnO_2 particles show similar shapes and sizes in both cases with well-defined facets and a limited growth in the direction perpendicular to the central axis.

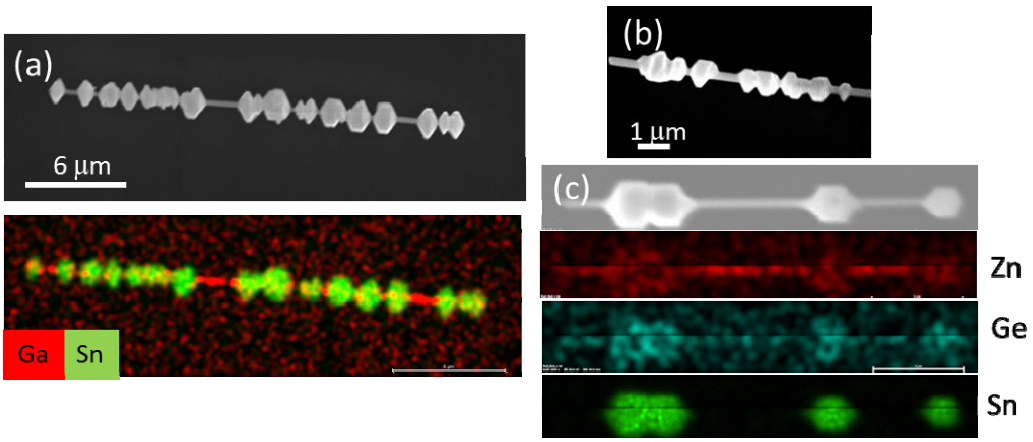

Figure 1. SEM images and elemental mappings of complex nanostructures based on a main oxide nanowire surrounded by SnO_2 particles. (a) Ga_2O_3/SnO_2 and (b-c) Zn_2GeO_4/SnO_2 nanostructures.

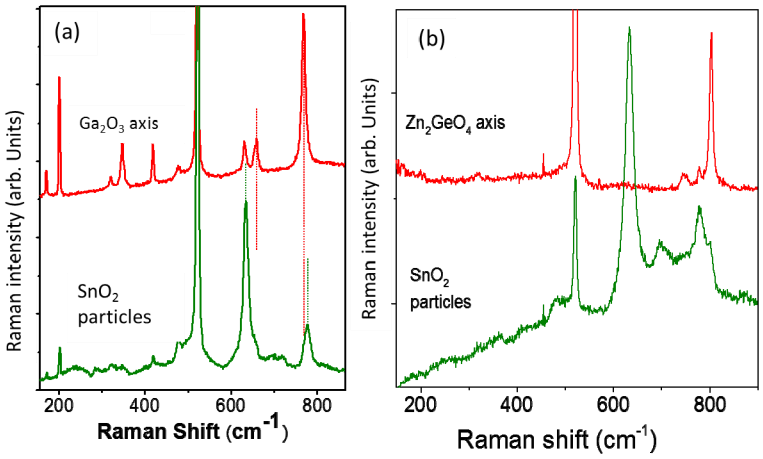

Figure 2. Raman characterization of (a) Ga_2O_3/SnO_2 and (b) Zn_2GeO_4/SnO_2 nanostructures.

In order to check the crystal quality of the oxide nanostructures, Raman spectra measurements have been done and summarized in Figure 2. Raman spectra from axial nanowires show a very good crystal quality in both nanostructures and characteristic modes of Ga_2O_3 and Zn_2GeO_4 are well-defined (upper curves in Figure 2). Raman spectra recorded from the attached particles are also shown (lower curves in Figure 2). SnO_2 crystallites on Ga_2O_3 nanowires exhibit better crystal quality than those on Zn_2GeO_4 nanowires, which could be due to the Ge and Zn co-doping of the particles. The 520 cm^{-1} peak presented in all Raman spectra corresponds to the silicon substrate.

Sn impurities have been proposed as a way to increase electrical n-type conductivity in some oxides nanowires. However, this is difficult to achieve because of the impurities out-diffusion during the growth process, which is sometimes difficult to prevent. Also, the addition of Sn to the source materials have been found to influence as well the shape of oxide nanowires obtained by thermal evaporation methods, leading to branched nanowires or to nanowires with higher aspect-ratio[4,11]. Here, we observe that once the main Ga_2O_3 or Zn_2GeO_4 nanowires are formed, the out-diffused Sn impurities may be aggregated at some sites of the lateral surface of the NWs and act as nucleation centers for SnO_2 particles.

Other impurity of interest in semiconducting oxides is chromium due to the intraionic red luminescence of Cr^{3+} cations. The quantum yield of red luminescence of Cr increases considerably when impurities are embedded in an oxide nanowire matrix instead of bulk material[12]. In a previous work on Cr doped Ga_2O_3 nanowires obtained after a two-step growth process, an intense red luminescence was achieved[4]. Also, the addition of both Sn and Cr to the precursors and a thermal treatment in a single step lead to the formation of a considerable amount of crossed Ga_2O_3/SnO_2 nanowires[9,10]. These structures consist of a main Ga_2O_3 axis where a certain number of crossed SnO_2 wires are grown. The formation of SnO_2 particles or wires around the axis has been discussed as a function of the orientation of the axis NW[10]. Here we present some nanostructures that have a high number of SnO_2 wires crossing the Ga_2O_3 nanowire, leading to a kind of "core-shell" morphology with a rather complex shell.

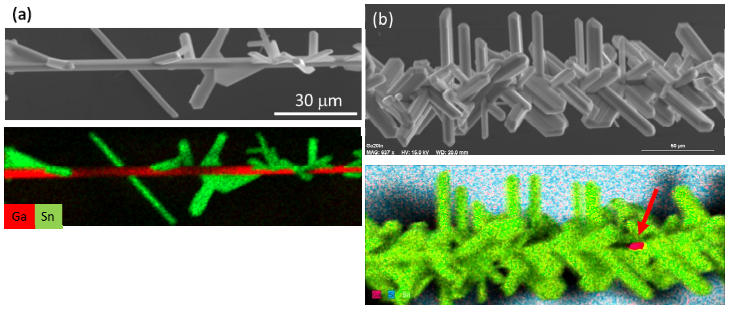

Figure 3. SEM and elemental mapping of Ga_2O_3 nanowires with different number of SnO_2 crossing wires.

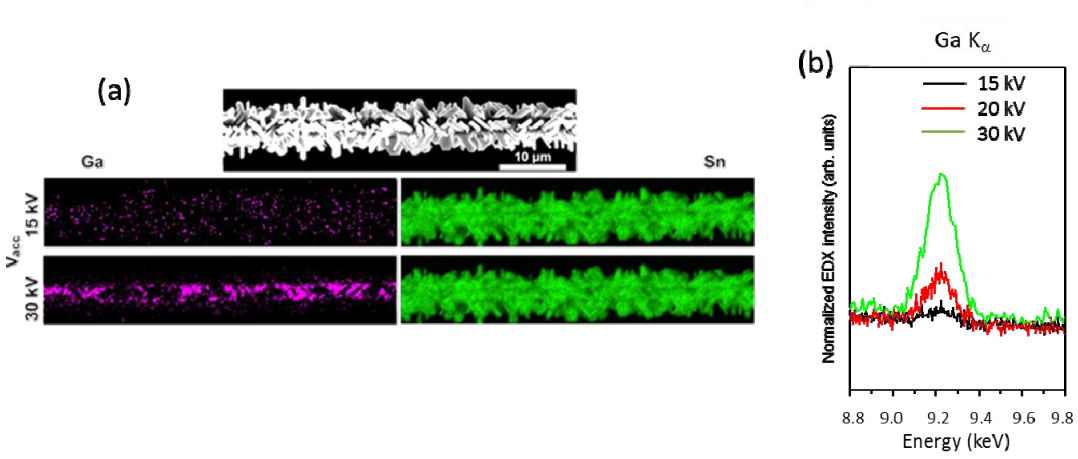

Figure 4. (a) SEM and EDX Ga and Sn mappings of complex core-shell Ga_2O_3/SnO_2 nanostructures analyzed at 15 kV and 30 kV acceleration voltages. (b) Short-range energy EDX spectra showing the Ga characteristic X-ray lines recorded at 15 and 30 kV.

Figure 3a shows a structure composed of a central Ga_2O_3 axis crossed by rather separated SnO_2 wires, while Figure 3b shows a more complex morphology. As the EDX mapping shows, Sn appears to cover fully the whole structure and just a short length of the axis remains uncoated (marked by an arrow in Fig. 3b). Figure 4a shows the EDX mappings for Ga and Sn of other of these fully coated nanowires at different acceleration voltages of the electron beam. Since the higher the energy of the electron beam, the larger the penetration depth, the results show that Ga is present at the core axis, as it can be seen in Fig. 4a (Ga mapping at 30 kV). Figure 4b shows partial EDX spectra of the characteristic K_α lines of Ga for 15, 20 and 30 kV acceleration voltages recorded from the central part of the structure. The penetration range of energetic electrons into a specimen, which beside the beam energy also depends on the material density and atomic number, can be simulated with CASINO program[12]. For pure Ga_2O_3, simulations of the electron paths until their thermalization yield a value of 500 nm for 10 kV and about 2 microns for 25 kV. Now we have to consider as well the SnO_2 shell that coats the Ga_2O_3 nanowire. We have carried out simulations by considering a SnO_2 shell of several thickness (from 500 nm to 2000 nm) surrounding the Ga_2O_3 core. The simulated profiles for electrons with energies of 15, 20 and 30 keV impinging a SnO_2 shell of 750 nm are shown in Figure 5. This depth is what better fits with experimental EDX results presented above (Fig.4). As it can be observed, electrons with 15 keV test a region less than 750 nm in depth, but electrons with 20 keV energy reach the Ga_2O_3 core, which would agree with the EDX signal detected in Figure 4b. These results suggest that the thickness of the SnO_2 coating the Ga_2O_3 axis would be around 750 – 1000 nm.

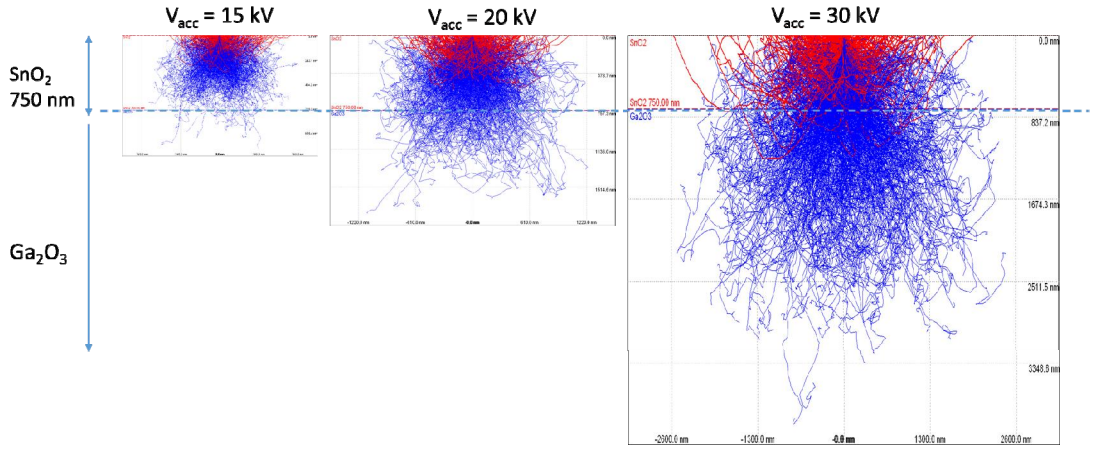

Figure 5. Montecarlo simulation (CASINO) electrons paths up until they stop (blue lines) within a sample composed of a first SnO_2 layer of 750 nm thickness and Ga_2O_3 below.

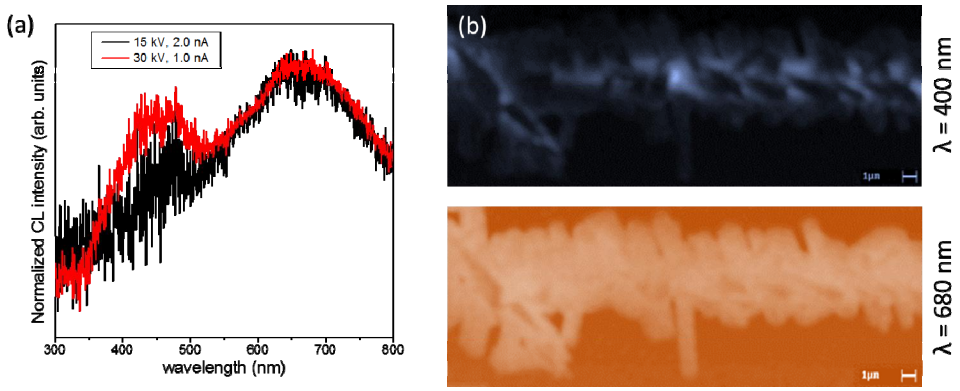

Figure 6. (a) CL spectra of one complex Ga_2O_3/SnO_2 structure recorded with electrons accelerated with energies of 15 and 30 keV. (b) Monochromatic CL images at 400 nm (upper image) and at 680 nm (lower image) of one complex Ga_2O_3/SnO_2 nanostructure, recorded at 30 keV.

One of the potential attractions of these nanostructures of mixed oxides is that different luminescent behavior is possible in the same nanostructure. We have carried out Cathodoluminescence (CL) measurements in the SEM, which enables high spatial resolution. Semiconducting oxides usually exhibit luminescence due to the radiative centers involving oxygen vacancies. Native defects in Ga_2O_3 originate a luminescence band in the UV-blue region[14-15]. On the other hand, SnO_2 show a complex luminescence band in the green-orange-red region with several components that is affected by oxygen vacancies and surface states of the crystal facets[16-17]. Figure 6a shows the CL spectra of one of these complex Ga_2O_3/SnO_2 structures (similar to that shown in Fig. 5) recorded with electron beam energies of 15 and 30 keV. The broad green band around 680 nm, which is characteristic of SnO_2, is observed in both cases, while the blue-UV band of Ga_2O_3 is only detected for 30 keV electron beam energy due to the higher penetration depth of electrons. Figure 6b shows two monochromatic CL images revealing areas emitting photons of 400 nm and 680 nm wavelengths. These selected wavelengths correspond to maxima of band emissions in Ga_2O_3 and SnO_2, respectively. The images clearly reveal the spatial distribution of the luminescence centers in the complex structure.

4. CONCLUSIONS

We have successfully grown complex nanostructures based on oxide semiconducting materials, such as Ga_2O_3, Zn_2GeO_4 and SnO_2, by a rather simple evaporation method. The complex structures consisted of a main oxide nanowire axis, to which either particles or rods were attached. Zn_2GeO_4 and Ga_2O_3 nanowires are the main axis and particles or rods are made of SnO_2. The quality of the structure was assessed by Raman spectroscopy, which shows the characteristic peaks of the corresponding lattices. In the case of SnO_2 rods grown on Ga_2O_3 nanowires, EDX microanalysis maps and CL measurements show that a core-shell structure is formed at the axis. Montecarlo simulations of the electron paths within the sample until they lose their energy agrees with a model of a shell of about 750 nm width for the SnO_2 that coat the main Ga_2O_3 axis. These results aim to shed some light on the understanding of the driving mechanisms that lead to the formation of complex oxide nanostructures.

5. ACKNOWLEDGMENTS

This work has been supported by MINECO (projects CSD 2009-2013, MAT 2012 - 31959, MAT 2015 – 65274 – R - FEDER). M. A-O acknowledges financial support from MEC (FPU contract).

REFERENCES

[1] Thelander C., Agarwal P., Brongersma S., Eymery J., Feiner L.F., Forchel A., Scheffler M., Riess W., Ohlsson B.J., Gösele U., Samuelson L., "Nanowire-based one-dimensional electronics" Materials Today, 9, 28-35 (2006).

[2] Hwang Y.J., Wu C.H., Hahn C., Jeong H.E., Yang P., "Si/InGaN Core/Shell Hierarchical Nanowire Arrays and their Photoelectrochemical Properties" Nano Lett., 12, 1678–1682 (2012).

[3] Yu X., Marks T.J., Facchetti A., Nature Mater. 15, 383-396 (2016).

[4] López I., Nogales E., Méndez B., Piqueras J., Peche A., Ramirez-Castellanos J., González-Calbet J., "Influence of Sn and Cr Doping on Morphology and Luminescence of Thermally Grown Ga_2O_3 Nanowires" J. Phys. Chem. C. 117, 3036-3045 (2013).

[5] Nogales E., Hidalgo P., Lorenz K., Méndez B., Piqueras J., Alves E., "Cathodoluminescence of rare-earth implanted Ga_2O_3 and GeO_2 nanostructures" Nanotechnol., 22, 285706 (2011).

[6] Hidalgo P., López A., Méndez B., and Piqueras J., "Synthesis and Optical Properties of Zn_2GeO_4 Microrods" Acta Materialia, 104, 84-90 (2016).

[7] Maestre D., Cremades A., Piqueras J., "Study of the morphology and luminescence of SnO_2 micro- and nanostructures synthesized by a two-step thermal process" J. Cryst. Growth, 311, 1212-1216 (2009).

[8] Vila M., Díaz-Guerra C., Piqueras J., López-Conesa L., Estradé S., Peiró F., "Growth, Structure and mechanical resonance of Bi_2O_3 nano and microwires" CrystEngComm. 17, 132 (2015).

[9] Martínez-Criado G., Segura-Ruiz J., Chu M.-H., Tucoulou R., López I., Nogales E., Méndez B., and Piqueras J., "Crossed Ga_2O_3/SnO_2 Multiwire Architecture: A Local Structure Study with Nanometer Resolution" Nano Letters, 14, 5479-5487 (2014).

[10] Alonso-Orts M., Sánchez A.M., Hindmarsh S.A., López I., Nogales E., Piqueras J., Méndez B., "Shape Engineering Driven by Selective Growth of SnO_2 on Doped Ga_2O_3 Nanowires" Nano Letters, 17, 515-522 (2017).

[11] Cebriano T., Méndez B., Piqueras J., "Sb_2O_3 microrods: self-assembly phenomena, luminescence and phase transition" J. Nanopart Res, 15, 1667 (2013).

[12] Nogales E., García J. A., Méndez B., Piqueras J., "Red luminescence of Cr doped Ga_2O_3 nanowires" J. Appl. Phys. 101, 033517 (2007).

[13] Drouin D., Couture A.R., Joly D., Tastet X., Aimez V., Gauvin R., "CASINO V2.42—A Fast and Easy-to-use Modeling Tool for Scanning Electron Microscopy and Microanalysis Users" Scanning 29, 92 (2007).

[14] Binet L., Gourier D., "Origin of the blue luminescence of β- Ga_2O_3" J. Phys. Chem. Solids, 59, 1241 (1998).

[15] Shimamura K., Víllora E. G., Ujiie T., Aoki K., "Excitation and photoluminescence of pure and Si-doped β-Ga_2O_3 single crystals" Appl. Phys. Lett. 92, 201914 (2008).

[16] Maestre D., Cremades A., Piqueras J., "Growth and luminescence properties of micro- and nanotubes in sintered tin oxide", J. Appl. Phys. 97, 044316 (2005).

[17] Das, S., Kar, S., Chaudhuri, S., "Optical properties of SnO_2 nanoparticles and nanorods synthesized by solvothermal process" J. Appl. Phys. 99, 114303 (2006).